

PACS numbers: 42.55.Lt; 42.60.Lh
DOI: 10.1070/QE2007v037n04ABEH013253

Efficient XeCl laser with a semiconductor opening switch in a pump oscillator: Theory and experiment

Yu.I. Bychkov, A.N. Panchenko, V.F. Tarasenko,
A.E. Tel'minov, S.A. Yampol'skaya, A.G. Yastremsky

***Abstract*. The parameters of laser radiation and kinetic processes of plasma formation and production of inverse population are studied. Electrophysical processes proceeding in a feed circuit containing a semiconductor opening switch and intermediate inductive energy storage are also considered. It is shown that the semiconductor opening switch controls the amount of energy in the inductive storage, and a high-voltage short prepulse with a peak pump power density of $\sim$1 MW cm^{-3} appearing during the current interruption can produce a volume-discharge plasma and create the inverse population for the time $\sim$10 ns, providing the conditions for efficient pumping of the active medium from the main capacitor. The time dependences of the pump and emission powers, the concentrations of electrons, excited xenon atoms, HCl(v) molecules in excited vibrational states and of the ionisation, recombination, and attachment rates are calculated. Kinetic processes determining the parameters of laser radiation are analysed. The output energy up to 1.0 J is obtained for 90-ns (FWHM) pulses with the efficiency up to 4.0 % with respect to the pump energy. The maximum output power was 11 MW for the lasing efficiency of 4.7 % with respect to the pump power. The calculated and experimental time dependences of the voltage across the laser gap, discharge current, and output power are in good agreement.**

Keywords: *semiconductor opening switch, formation of a plasma and inverse population, efficient excitation.*

1. Introduction

Electric-discharge-pumped noble-gas-halide exciplex lasers are the most powerful UV lasers and are applied in a variety of fields in science and technology. The optimisation of pumping and the choice of the electric circuit for such lasers are quite complicated. The requirements to the electric circuit are determined by physical processes involved in the preparation of the active medium and the conditions of optimal pumping. At the first stage, after the application of a voltage to electrodes, the self-sustained-discharge plasma is formed and the electron concentration increases up to $\sim 10^{11}$ cm^{-3}. At the second stage, the active medium is produced and the electron concentration achieves 10^{15} cm^{-3}. Lasing is still absent at this stage, and therefore the energy spent to produce the active medium reduces the laser efficiency. At the third stage lasing appears. The qualitative description of physical processes at these three stages allows us to formulate the requirements to a feed circuit.

To provide the spatial homogeneity of a self-sustained discharge, it should be formed at the maximal initial strength of the electric field at electrodes [1]. To produce the active medium, a high electron concentration is required, which is achieved due to efficient ionisation and excitation at a high peak pump power density (up to $\sim 10^6$ W cm^{-3}). To increase the laser efficiency, the duration of an electric pulse producing the plasma and active medium should be minimal. The duration of the emission pulse during pumping of the active medium depends on the pump power. To increase the emission pulse duration, a low pump power is required, while to increase the pump efficiency, it is necessary to match the wave resistance of the circuit with the electric resistance of the discharge plasma [2].

The problem of the choice of the efficient scheme for pumping a XeCl laser is that two electric pulses are needed (double-discharge pumping) whose parameters cannot be simply obtained. In this paper, we pumped a XeCl laser by a double discharge by using an electric feed circuit with a semiconductor opening switch. A detailed analysis of the results taking into account kinetic processes in the plasma and electrophysical processes in the electric circuit shows that such a scheme can provide the efficient pumping of the XeCl laser.

We used an inductive storage with a plasma-erosion opening switch to pump a XeCl laser for the first time in [3]. Studies on the application of inductive energy storages for pumping lasers were continued after the advent of semiconductor opening switchs (SOS diodes) and generators based on them [4]. The outlook for using this method for efficient pumping of HF, CO_2, and N_2 lasers was demonstrated in [5].

In [6], the inductive energy storage with a semiconductor opening switch was first successfully applied to produce a discharge in an excimer XeCl laser. Pulsed lasing with a pulse duration of $\sim$450 ns was obtained. The duration of pulses emitted by XeF and KrF lasers was considerably increased upon pumping them by using a SOS diode opening switch [7]. Kinetic processes in a long-pulse XeCl laser, in which a prepulse was formed by means of a semiconductor opening switch, were simulated in [8].

Yu.I. Bychkov, A.N. Panchenko, V.F. Tarasenko, A.E. Tel'minov, S.A. Yampol'skaya, A.G. Yastremsky Institute of High-Current Electronics, Siberian Branch, Russian Academy of Sciences, prosp. Akademicheskii 2/3, 634055 Tomsk, Russia;
e-mail: alexei@loi.hcei.tsc.ru, VTF@loi.hcei.tsc.ru, bichkov@lgl.hcei.tsc.ru

Received 16 May 2006; revision received 10 October 2006
Kvantovaya Elektronika **37** (4) 319 – 324 (2007)
Translated by M.N. Sapozhnikov

In this paper, we studied in detail kinetic processes at three successive stages: the formation of the plasma, and the production and pumping of the active medium. In addition, we analysed the potential possibilities of the feed circuit with a semiconductor opening switch.

2. Electric circuit of the XeCl laser and the plasma model

2.1 Electric circuit

Figure 1 presents the electric circuit used to simulate the XeCl laser. The circuit consists of four electric circuits and the following elements: three capacitors ($C_1 - C_3$); four inductances ($L_1 - L_4$) corresponding to each of the circuits, the resistance R_{pl} of the plasma in a gas-discharge gap, which is an active nonlinear resistance for the electric circuit; the spark-preionisation-gap resistance R_{sp}; the spark-gap resistance R_{sw} commuting the main capacitor C_1; and the semiconductor opening switch (SOS diode) R_d switching a current in the inductance L_1 to charge the peaking capacitor C_2.

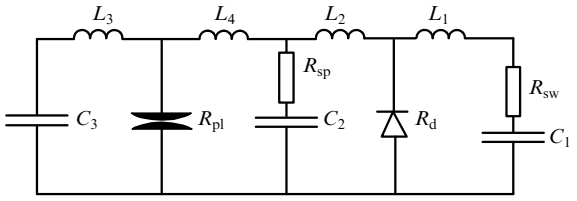

Figure 1. Equivalent electric pump circuit used in calculations: R_{pl}, R_d, R_{sw}, and R_{sp} are resistances of the discharge plasma, SOS diodes, spark gap, and spark preionisation gaps, respectively; $C_1 = 70$ nF, $C_2 = 2.45$ nF, $C_3 = 10$ nF; $L_1 = 30$ nH, $L_2 = 2$ nH, $L_3 = 3$ μH, $L_4 = 5$ nH.

The active volume V of the laser was 430 cm^3, the interelectrode gap was 4 cm, the discharge region width and length were 1.5 and 72 cm, respectively. The profile of electrodes made of a stainless steel was nearly cylindrical with a radius of 40 mm. The laser resonator was formed by dielectric mirrors with the reflection coefficients 100 % and 30 % (at 308 nm). The Ne : Xe : HCl = 2660 : 24 : 3 Torr gas mixture was used.

The capacitor C_1 was the main energy storage for pumping the active medium. The control capacitor C_3 provided the preliminary flow of the current through diodes in the forward direction. The charging voltage for this capacitor was only 12 kV, i.e. the energy spent to control the opening switch was less than 1 J. The capacitor C_2 was used to obtain a high peak power at the initial stage of a discharge. Ten special SOS diodes placed in parallel with peaking capacitors were used as the semiconductor opening switch. The operation of diodes in the regime of the opening switch was achieved by transmitting preliminary 100 – 500-A current through them in the forward direction for ~500 ns. As a result, the diodes acquired the property to transmit the current in the backward direction. When the inverse current achieved a certain value, the resistance of the diode increased by more than an order of magnitude for a short time (10 – 15 ns).

Figure 2 shows the experimental time dependence of the resistance of the opening switch. This dependence was used in the program for calculations. The program also takes in

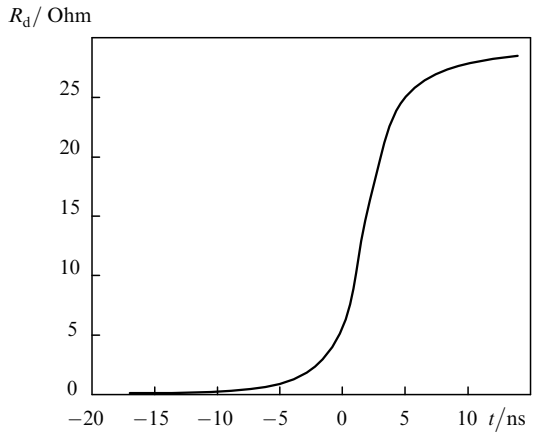

Figure 2. Time dependence of a SOS diode resistance.

into account the possible change in the voltage polarity on diodes at any instant of pumping. In this case, the diode resistance decreases and current passes through diodes in the forward direction.

Before switching on the circuit, the capacitors C_1 and C_3 were charged up to voltages of opposite polarities. The choice of the polarity was determined by the condition at which the discharge current of the capacitor C_3 flows through diodes in the forward direction. The capacitor C_3 was discharged through the inductances L_4, L_3, and L_2 and SOS diodes, by producing their direct pumping. At the instant of the complete recharge of the capacitor C_3, the synchronisation circuit switched on the gap of the main capacitor C_1, which began to discharge through the inductance L_1 and SOS diodes in the backward direction. For the time during which the diode resistance for the inverse current remains small, energy was accumulated in the inductance L_1. After a drastic increase in the diode resistance, the inductive current was switched over to charging the capacitor C_2.

The charging circuit of the capacitor C_2 contains spark gaps of UV preionisation, which produced the initial concentration of electrons in the gas gap. The formation of the plasma and an increase in its conduction were observed already during the rise of the voltage across the capacitor C_2. As the discharge current was further increased, the peaking capacitor rapidly discharged through the plasma and the active medium was produced. Then, pumping was performed during the discharge of the main capacitor C_1.

2.2 Plasma model

The self-consistent kinetic model of a XeCl laser is based on the local electric field approximation and includes the Boltzmann equation for electrons, the system of rate equations for concentrations of plasma particles and equations for the external electric circuit. The distribution of the laser photon flux along the optical axis was described by the one-dimensional resonator model [9]. It was assumed in calculations that the discharge was spatially homogeneous.

The kinetic model contains more than 250 reactions and coincides as a whole with the model used in [10]. For the neon atom and its first ion, the following levels were considered: Ne (ground state), Ne*(3s), Ne** (all other excited states), and Ne$^+$ (the ground state of the ion). For the xenon atom and ion, the following levels were consid-

ered: Xe (ground state), three excited states $Xe^*(6s)$, $Xe^{**}(6s', 6p$, and $5d)$ and Xe^{***} (other excited states), and the ground state of the Xe^+ ion. The energy level diagram of HCl molecules contained the ground state HCl (0), three excited vibrational states HCl ($v = 1, 2, 3$), two excited electronic states HCl^* and HCl^{**} and the ground state of the molecular HCl^+ ion.

The energy level diagram of the excimer XeCl molecule contained the ground state XeCl(X) and excited states $XeCl^{**}$ of the molecule with the energy close to the dissociation energy. Each of the excited states XeCl(B) and XeCl(C) included two levels: XeCl (B, $v = 0$), XeCl (B, $v > 0$), and XeCl (C, $v = 0, 1$), XeCl (C, $v > 2$). In addition, the model took into account hydrogen atoms, chlorine atoms in the ground (Cl) and excited (Cl^*) states, H_2 molecules, the Ne_2^* and Xe_2^* dimers, Xe_2Cl molecules, molecular ions Ne_2^+, Xe_2^+ and $NeXe^+$, negative Cl^- ions, electrons and laser photons.

The system of rate equations for the concentration of plasma particles and equations for the electric circuit were solved by the Gear method, and the Boltzmann equation for electrons was solved by the method of weighted residuals [11].

3. Experimental and calculated results

We measured in experiments the voltage across the peaking capacitor C_2 (with an ohmic voltage divider), the discharge current (with a Rogowski loop), and the time dependence of the laser output power (with a FEK-22SPU photodiode). The photodiode was located at a distance of 1 m from the output mirror. Radiation from the laser aperture was reflected to the photocathode by a quartz plate and was attenuated by metal grids to provide the photocathode operation in the linear regime. Electric signals were recorded with a TDS-224 digital oscilloscope. The output laser energy focused with a quartz lens was measured with an IMO-2N calorimeter. The measurement errors did not exceed 15 %.

Pump regimes were studied for different charging voltages U_0 of the main inductive storage C_1. The main experimental parameters of the four pump regimes are presented in Table 1.

3.1 Comparison of experimental and calculated data

Figures 3 and 4 show the experimental and calculated time dependences of the voltage across the peaking capacitor, the discharge current, and the output laser power for the charging voltage of 36 kV. The first narrow peak of the experimental dependence of the voltage across the capacitor C_2 is caused by the breakdown of the spark preionisation gaps. At the instant of the current interruption, the inductive storage forms a

Table 1. Main parameters of the four pump regimes of the XeCl laser.

$U_0(C_1)$/ kV	U_{br}/kV	$I(C_2)$/ kA	$I(C_1)$/ kA	t_{del}/ns	Q_{las}/J	P_{peak}/ MW	$t_{1/2}$/ns
25	52	4	16	87	0.44	6	77
30	63	13	21	60	0.63	7.5	82
33	68	22	26	40	0.82	9.5	85
36	71.5	28	31	35	1.00	11.5	90

Note: U_{br}: breakdown voltage; $I(C_2)$: peak discharge current of peaking capacitors; $I(C_1)$: peak discharge current of the storage capacitor; t_{del}: delay time of the laser pulse with respect to the discharge-ignition time; Q_{las}: output laser energy; P_{peak}: peak laser power; $t_{1/2}$: laser pulse FWHM for different U_0.

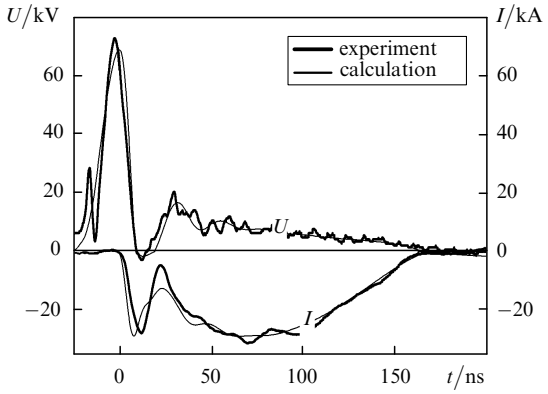

Figure 3. Experimental and calculated time dependences of the discharge current and voltage for the peaking capacitor.

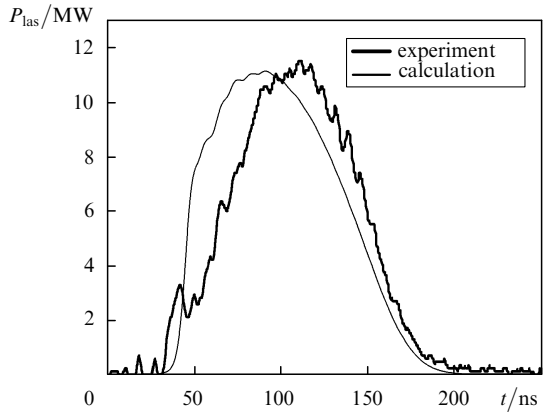

Figure 4. Experimental and calculated time dependences of laser radiation power.

prepulse with the amplitude $U_{max} = L_1 dI/dt \sim 70 - 80$ kV, where dI/dt is the rate of current interruption in diodes with the rise time of about 20 ns. After the laser-gap breakdown, the discharge current rapidly increases and a short high-power pump pulse is formed. A combined action of such factors as a high breakdown voltage and a drastic increase in the discharge current, when the inductive energy storage is used, considerably improves the homogeneity of the discharge in the working mixtures of exciplex lasers and makes it more stable [5–7, 12]. Then, the main energy is supplied to the active medium of the laser during the discharge of the capacitor C_1. For a large value of U_0, the mismatch between the impedance of C_1 and the discharge resistance can be observed. However, all the subsequent current oscillations pass through the SOS diodes, reducing the erosion of electrodes and improving the reliability of the laser [6].

Double-discharge pumping by a generator with the inductive energy storage is similar to the diode-mode regime in the schemes of excitation by a double discharge with spark gaps [2] and magnetic switches [13, 14]. However, the inductive generator does not require the pulsed charging of capacitors and precise synchronisation between the prepulse generator and the main energy storage. In addition, when a laser operates in the diode-mode regime, a pause often appears between the instant of the laser-gap breakdown and the onset of pumping by the main energy storage, which can induce the development of inhomogeneities in the discharge. When the inductive energy storage is used, the current pause is absent.

The switching on of illumination was neglected in calculations and therefore the calculated voltage increases monotonically. The calculated and experimental dependences of the pulse duration and amplitude, the onset and termination of lasing are in good agreement. The calculations also quite accurately describe oscillations of the discharge current and voltage.

The calculated and experimental dependences of the output energy and efficiency of the laser on the charging voltage are also in good agreement (Fig. 5). The discrepancies lie within experimental errors and errors related to the assumptions adopted in the model. We calculated the energy supplied to the gas during the first half-period of the discharge current of the capacitor C_1. The maximum efficiency of the laser with respect to the energy supplied to the active medium was 4 % which is close to the maximum efficiency of a XeCl laser obtained upon double-discharge pumping [2, 12, 13]. The efficiency of energy transfer from the capacitor C_1 to the active medium of the laser proved to be low, being only $\sim$55 % for the 36-kV charging voltage. The energy lost in the active resistances of spark illumination gaps and diodes of the opening switch was $\sim$36.4 %. About 8.6 % of the stored energy remains in capacitors and inductances during the second half-period of the current. After the change of the voltage polarity across the capacitor C_1, diodes begin to transmit current in the forward direction (with a low resistance) and the current ceases in the plasma. The energy is supplied to the plasma only during the first half-period of pumping. To increase the total efficiency of the laser, it is necessary to reduce energy losses first of all in diodes of the opening switch.

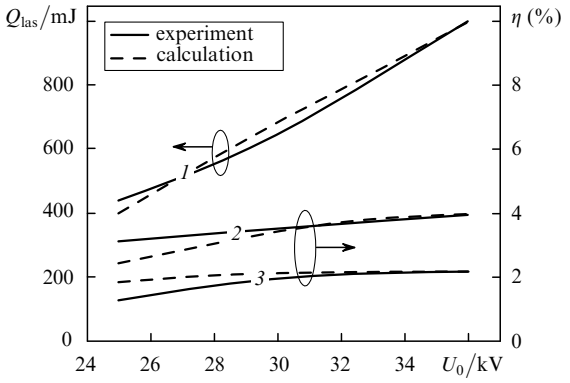

Figure 5. Experimental and calculated dependences of the laser radiation energy (*1*), the lasing efficiency with respect to the supplied energy (*2*), and the lasing efficiency with respect to the stored energy (*3*) on the charging voltage of the capacitor C_1.

3.2 Calculation results and discussion

Consider the pump regime with a charging voltage of 36 kV in more detail. Figure 6 presents the calculated time dependences of the pump power and output laser power. The peak power of 0.34 GW (0.81 MW cm^{-3}) at the instant $\sim$4 ns is produced by discharging the capacitor C_2 through a gas mixture. By the time of 17 ns, the pump power decreases approximately by a factor of four. Then, pumping is performed by discharging the main capacitor C_1, the maximum pump power achieving 0.23 GW (0.56 MW cm^{-3}). Figure 6 also shows the output radiation power whose maximum value

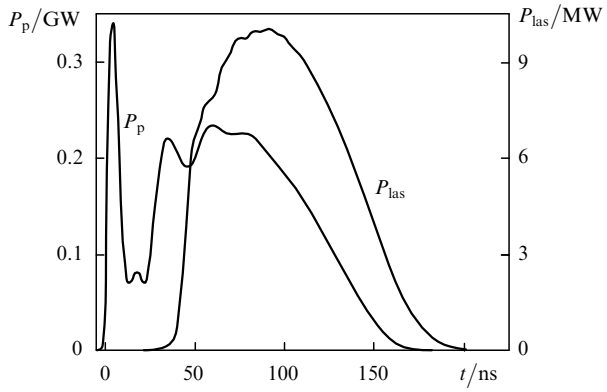

Figure 6. Calculated time dependences of the pump power P_p and laser radiation power P_{las} obtained at the charging voltage of 36 kV.

achieves 11.2 MW. The lasing efficiency with respect to the pump power is 4.7 %, which is a high value for XeCl lasers.

Figure 7 shows the calculated time dependences of the gain and absorption coefficient of the active medium. The gain is proportional to the concentration of XeCl molecules (B, $v = 0$), which are produced in a number of kinetic processes determining the difference between the time dependences of the pump power and gain and, in particular, the delay time of the gain maximum with respect to the pump power maximum. Thus, the first maximum of the gain equal to 4%·cm^{-1} is caused by the first peak of the pump power and corresponds to the time 19 ns. The delay of the gain maximum with respect to the pump maximum is $\sim$15 ns. Analysis of the gain dynamics shows that the active medium is already produced by the time of 19 ns and induced radiation is amplified; however, the density of laser photons is still very low ($\sim 10^{10}$ cm^{-3}). The pump power from the discharging capacitor C_2 at this instant becomes minimal (Fig. 6), while the main pump power from the discharging capacitor C_1 has still no time to increase. The second maximum of the gain equal to 3.6 %·cm^{-1} is caused by the discharge of the main capacitor C_1. By the time of 36 ns, the density of laser photons increases up to $\sim 10^{13}$ cm^{-3} (Fig. 8). This results in the saturation of the radiation flux, thereby reducing the gain.

Laser photons are absorbed during their interaction with the negative Cl^- ions (the photodetachment reaction), excited Xe^* atoms (photoionisation), and molecules Xe_2^+, Xe_2Cl, and Xe_2^* (dissociation of molecules). A greater part of laser photons is lost in electron photodetachment

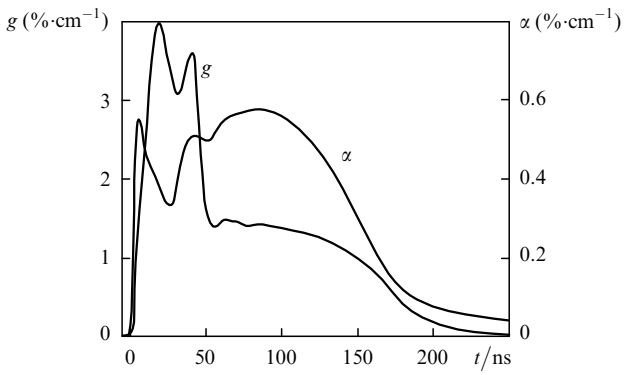

Figure 7. Calculated time dependences of the gain g and absorption coefficient α at 308 nm in the active medium of the XeCl laser.

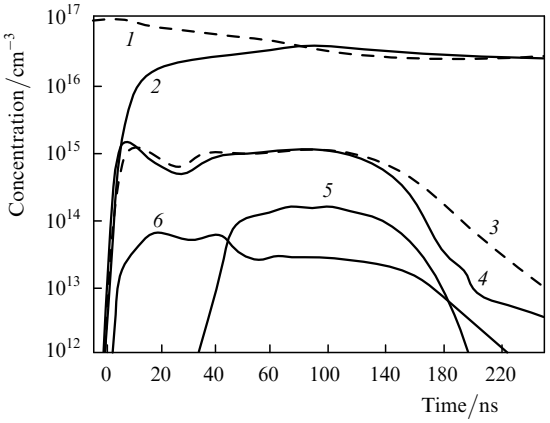

Figure 8. Calculated time dependences of the concentration of the main components of the plasma: HCl(0) (*1*), HCl ($v = 1, 2, 3$) molecules in excited vibrational states (*2*), excited xenon atoms (Xe^*, Xe^{**}, Xe^{***}) (*3*), electrons (*4*), laser photons (*5*), and XeCl (B, $v = 0$) molecules at the upper laser level (*6*).

reactions and upon photoionisation of excited Xe^* atoms. The absorption coefficient in the region of the maximum gain is an order of magnitude lower than the gain. The time profile of the absorption coefficient (Fig. 7) proves to be complicated and is determined in fact by the behaviour of the electron concentration, which governs variations in the concentrations of absorbing atoms and molecules.

Figure 8 shows the time dependences of the electron concentration, the total concentration of excited xenon atoms, the concentration of HCl(0) molecules, the total concentration of HCl($v = 1, 2, 3$) molecules in excited vibrational states, the concentration of XeCl(B, $v = 0$) molecules, and the density of laser photons. The time dependences of these concentrations characterise the basic physical processes determining laser pumping.

Already at the initial stage, by the time of 9 ns, the electron concentration of 1.3×10^{15} cm^{-3} is produced. Such a high concentration was achieved due to a high peak pump power produced by a semiconductor opening switch and the energy stored in the inductance of the main circuit. The concentrations of HCl($v = 1, 2, 3$) molecules in excited vibrational states increase simultaneously with a rapid increase in the electron concentration. This results in the increase in the rate of electron attachment processes. The production rate of highly excited $XeCl^*$ molecules is virtually equal to the electron attachment rate. The concentration of XeCl(B, $v = 0$) molecules produced upon relaxation of $XeCl^{**}$ molecules determines the gain in the active medium. The time dependence of the gain is similar to that of the concentration of XeCl(B, $v = 0$) molecules. By the time of 38 ns, a high rate of the increase in the density of laser photons causes a decrease in the concentration of XeCl(B, $v = 0$), thereby reducing the gain. Figure 8 also shows the time dependence of the concentration of excited xenon atoms. The concentration of excited xenon atoms is comparable with the electron concentration.

The rate of increase in the concentration of HCl($v = 1, 2, 3$) considerably affects the properties of the plasma and laser radiation. The attachment constants of electrons interacting with HCl($v = 1, 2, 3$) molecules are approximately 60 times higher than those for electrons interacting with HCl(0) molecules. An increase in the concentration of HCl($v = 1, 2, 3$) provides the required growth rate of the concentration of XeCl(B, $v = 0$). The maximum output radiation energy, which can be obtained after excitation of all HCl(0) molecules to the vibrational states HCl ($v = 1, 2, 3$), depends on the initial concentration of HCl(0). In the given regime, the total concentration of HCl(0) and HCl($v = 1, 2, 3$) molecules in a gas by the instant of pump pulse end is equal to 60 % of the initial concentration of HCl(0) molecules. This means that the increase in the pump pulse power and duration can increase the output power.

Figure 9 presents the calculated time dependences of the rates of direct and step ionisation and the attachment and recombination of electrons. These dependences determine the rates of creation and loss of electrons and their variation during pumping. Processes proceeding until the instant of time 33 ns are caused by peak pumping from the peaking capacitor. After 33 ns, the rates of processes are determined by the pumping of the gas by the energy from the main capacitor.

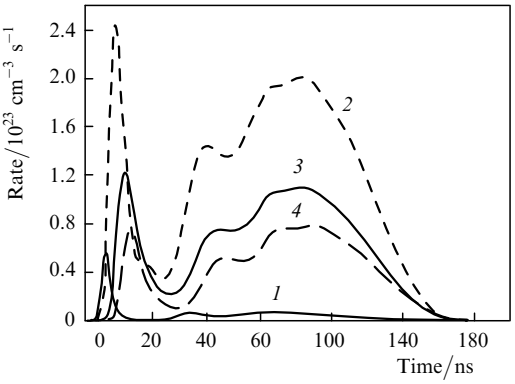

Figure 9. Calculated time dependences of the rates of the main processes of creation and loss of electrons: the direct ionisation rate (*1*), the total rate of step ionisation of excited Xe^* atoms (*2*), the total rate of dissociative electron attachment (*3*), and the total recombination rate (*4*).

Direct ionisation favours the increase in the electron concentration only at the initial stage of the discharge. As the concentrations of electrons and excited xenon atoms increase, the rate of step ionisation increases. By the time of 3 ns (at the electron concentration $\sim 10^{14}$ cm^{-3}), the rates of direct and step ionisation become comparable. A decrease in the electric field strength in the plasma reduces the rate of direct ionisation. In this case, the rate of step ionisation continues to increase and the further increase in the electron concentration is completely provided by step ionisation. Thus, the rate of step ionisation by the time 6 ns is 2.4×10^{23} cm^{-3} s^{-1}, while the rate of direct ionisation is 20 times lower. In the plasma, direct ionisation passes to step ionisation, which qualitatively changes the plasma properties. The increase in the electron concentration upon a strong decrease of the electric field strength in the plasma is provided only by step ionisation.

Note that the increase in the recombination and attachment rates at the initial stage of the discharge delays with respect to the increase in the step ionisation rate. Therefore, the pump power is mainly spent to produce electrons and excited Xe^* atoms, whose concentrations rapidly increase.

The rate of direct ionisation at the main pump stage remains very low and does not affect the increase in the

electron concentration. A high electron concentration is produced by step ionisation. It is typical for this stage that the concentrations of electrons and Xe^* in the range $33-133$ ns change only slightly, remaining at the level of $\sim 10^{15}$ cm^{-3}, whereas the rates of step ionisation, attachment, and recombination in this time interval change considerably. The situation appears when the rate of step ionisation in this time interval remains approximately equal to the sum of the attachment and recombination rates. The time dependences of the ionisation, attachment, and recombination rates depend on the distribution of the energy supplied into the active medium in various kinetic processes. A detailed study of the rates of processes and the distribution of the pump power among various plasmochemical channels is the subject of further independent investigations.

4. Conclusions

Based on calculations and experimental data, we have analysed kinetic processes determining the pumping of an electric-discharge XeCl laser with a feed circuit containing a semiconductor opening switch. The main conclusions are as follows.

(i) The best laser parameters were obtained for the charging voltage equal to 36 kV. The output energy was 1.0 J, the output power was 11.2 MW, the lasing efficiency with respect to the energy supplied to the active medium was 4 %, and the lasing efficiency with respect to the pump power was 4.7 %. This lasing efficiency is close to the maximum efficiency of the XeCl laser achieved upon double-discharge pumping and electron-beam pumping.

(ii) As the charging voltage of the storage capacitor is increased, the peak and main pump power increase, the delay time of the laser pulse decreases, and its duration increases. For the charging voltage of 36 kV, the maximum peak pump power density was 0.8 MW cm^{-3}, the initial electric field strength in the plasma was 18 kV cm^{-1}, and the delay time of the laser pulse with respect to the pump pulse was 35 ns.

(iii) It follows from the analysis of the ionisation, recombination, and attachment rates that, to produce the active medium with the gain providing the minimal delay time of the laser pulse with respect to the pump pulse, the prepulse should provide a pump power density of $\sim 10^6$ W cm^{-3}. The duration of the prepulse providing the plasma formation and creation of the active medium should be minimal in order to reduce the energy spent for the plasma formation.

(iv) Calculations revealed the following energy distribution at the 36-kV charging voltage: the energy stored in the main capacitor was 45.3 J, the energy supplied to the active medium was 25.1 J, and the energy remained in the circuit after pumping was 3.9 J. The energy losses in spark illumination gaps, and the opening switch were 16.3 J. The efficiency of energy transfer from the initial inductive storage to the gas was 55 %.

(v) The consumption of HCl molecules during pumping was ~ 40 %, so that it is possible to increase the output energy by increasing the pump power and (or) the pump pulse duration.

(vi) Our study has shown that a semiconductor opening switch can be used to control the energy stored in the inductive storage, while the high rate of the current interruption provides the required peak power at the short pulse duration. The properties of radiation from a XeCl laser can be improved by improving the parameters of the interrupter and reducing first of all energy losses.

Acknowledgements. This work was supported by the International Science and Technology Center (Project No. 2596).

References

1. Bychkov Yu.I., Yampolskaya S.A., Yastremsky A.G. *Laser Particle Beams*, **21**, 233 (2003).
2. Long W.H., Plummer J., Stappaerts E.A. *Appl. Phys. Lett.*, **43** (8), 735 (1983).
3. Mesyats G.A., Panchenko A.N., Tarasenko V.F. *Dokl. Akad. Nauk SSSR*, **307** (4), 869 (1989).
4. Rukin S.N. *Prib. Tekh. Eksp.*, **4**, 5 (1999).
5. Baksht E.H., Panchenko A.N., Tarasenko V.F. *IEEE J. Quantum Electron.*, **35** (3), 261 (1999).
6. Baksht E.H., Panchenko A.N., Tarasenko V.F. *Kvantovaya Elektron.*, **30** (6), 506 (2000) [*Quantum Electron.*, **30** (6), 261 (2000)].
7. Baksht E.H., Panchenko A.N., Tarasenko V.F., Matsunaga T., Goto T. *Jap. J. Appl. Phys.*, **41**, 3701 (2002).
8. Bychkov Yu.I., Baksht E.H., Panchenko A.N., Tarasenko V.F., Yampolskaya S.A., Yastremsky A.G. *Proc. SPIE Int. Soc. Opt. Eng.*, **4747**, 99 (2001).
9. Jonson T.H., Palumbo L.J., Hunter A.M. *IEEE J. Quantum Electron.*, **15**, 289 (1979).
10. Riva R., Legentil M., Pasquiers S., Puech V. *J. Phys. D: Appl. Phys.*, **28**, 856 (1995).
11. Fletcher C.A.J. *Computational Galerkin Methods* (New York: Springer, 1984).
12. Makarov M., Bonnet J., Pigache D. *Appl. Phys. B*, **66**, 417 (1998).
13. Fischer C.H., Kushner M.J., DeHart T.E., MacDaniek J.P., Petr R.A., Ewing J.J. *Appl. Phys. Lett.*, **48**, 1574 (1986).
14. Trentelman M., Peters P.J.M., Mei Q.-C., Witteman W.J. *J. Opt. Soc. Am. B*, **12**, 2494 (1995).